

Joseph D. Bruton · Abram Katz · Jan Lännergren ·
Fabio Abbate · Håkan Westerblad

Regulation of myoplasmic Ca²⁺ in genetically obese (*ob/ob*) mouse single skeletal muscle fibres

Received: 27 February 2002 / Accepted: 27 May 2002 / Published online: 29 June 2002
© Springer-Verlag 2002

Abstract The present study examined whether calcium handling in skeletal muscle fibres from *ob/ob* mice was abnormal compared to normal mice. Simultaneous measurements of free myoplasmic calcium and force were made in mouse single intact muscle fibres at rest, during repetitive stimulation and for 30 min afterwards. Fibres were subjected to two bouts of intermittent tetanic contractions 1 h apart. The first bout consisted of 50 tetani only, while during the second bout stimulation was continued until force fell to 40% of control. During a bout of 50 repeated contractions, muscle fibres from *ob/ob* mice were unable to maintain basal calcium and tetanic calcium transients. During a second series of contractions, muscle fibres from *ob/ob* mice showed a marked improvement in calcium handling compared to the first series but still fatigued more rapidly than control fibres. It is concluded that calcium handling in skeletal muscle fibres from *ob/ob* mice is abnormal compared to fibres from normal mice and this contributes to premature fatigue.

Keywords Calcium · Contraction · Diabetes · Exercise · Insulin · Muscle fatigue ·

Introduction

Genetically obese mice that lack leptin (*ob/ob* mice) and streptozotocin (STZ) injected rodents have been used as animal models of type 2 and type 1 diabetes respectively [9, 20, 27]. In isolated whole muscle preparations from diabetic animals, force declines more quickly during repeated contractions than in muscles from control animals, i.e. diabetic muscle has a reduced endurance

([10, 22, 23] but see [31]). In addition, muscles from diabetic animals generate contractions that are smaller and have longer time courses than those from normal animals [9, 23, 31]. It has been speculated that altered contractile function in diabetic muscle may reflect impaired intracellular Ca²⁺ homeostasis, in particular its release and re-uptake by the sarcoplasmic reticulum (SR) [10, 31]. Indeed, abnormal Ca²⁺ homeostasis has been implicated in insulin resistance in various tissues (for review see [21]). However measurement of Ca²⁺ uptake by SR isolated from diabetic skeletal muscle has not given a definitive answer with both increases [16] and reductions reported [14]. Only one study to date has addressed the question of Ca²⁺ handling by intact skeletal muscle cells from mouse models of diabetes. That study reported that in muscle isolated from agouti mice, resting free myoplasmic [Ca²⁺]_i ([Ca²⁺]_i) was elevated compared to that measured in normal muscle cells [35]. In addition, there was a greater influx of ⁴⁵Ca²⁺ in insulin-resistant muscle compared to control muscle which suggests that the sarcolemma was more permeable to Ca²⁺.

Thus, at the moment there is little information regarding Ca²⁺ homeostasis in intact skeletal muscle fibres of *ob/ob* mice or other models of insulin resistance or diabetes. The aim of this study was to examine Ca²⁺ handling in skeletal muscle fibres in *ob/ob* compared to normal mice and determine if the altered force and time-course of contractions in muscle from *ob/ob* animals was due in part to abnormalities in Ca²⁺ handling. It was found that at rest basal [Ca²⁺]_i and tetanic Ca²⁺ transients were not significantly different in intact single muscle fibres of *ob/ob* and normal mice. However, during a bout of repeated contractions, muscle fibres from *ob/ob* mice were less able than those from normal mice to maintain basal [Ca²⁺]_i and tetanic Ca²⁺ transients.

J.D. Bruton (✉) · A. Katz · J. Lännergren · F. Abbate ·
H. Westerblad

Department of Physiology and Pharmacology, Karolinska Institutet,
von Eulers väg 4, 171 77 Stockholm, Sweden
e-mail: joseph.bruton@fyfa.ki.se
Tel.: +46-8-7287254
Fax: +46-8-327026

Materials and methods

Animals and preparations

Young (3–5 months) C57BL genetically obese male mice (*ob/ob*) and their wildtype counterparts (WT) were supplied by B & K

Universal, Sollentuna, Sweden. Mice were killed by rapid neck disarticulation. Extensor digitorum longus (EDL) and flexor digitorum brevis muscles were removed. These studies were approved by the local ethics committee.

Whole muscles

Metal clips were attached to the tendons and the EDL muscle was suspended horizontally between an adjustable hook and a laboratory-built force transducer in a Perspex muscle bath. The muscle preparations were flanked by platinum electrodes, which were used for stimulation. Muscles were stretched to the length where maximum tetanic force (P_0) was obtained. For each muscle, a control force–frequency curve was obtained by giving 500-ms tetani between 1 Hz and 150 Hz at 1-min intervals and plotting the peak force against the frequency. Force–frequency curves reveal gross differences in force production which might indicate differences in Ca^{2+} handling. After a 15-min rest period, the muscle was subjected to 50 tetani (300 ms, 70 Hz) applied at 2-s intervals. Thirty minutes afterwards, a second force–frequency curve was obtained. The length of the EDL muscle in the muscle bath was measured and the muscle was removed and gently blotted on tissue paper to remove excess fluid and then weighed. The cross-sectional area of the EDL muscle was estimated using muscle length and weight and assuming a specific gravity of 1.06 mg ml^{-1} .

Single muscle fibres

Single fibres were mechanically isolated from the flexor digitorum brevis muscles. Platinum clips were attached to the tendons and the fibres were suspended horizontally between an adjustable hook and a force transducer (Akers AE 801) in the perfusion channel of a muscle chamber. The diameter of the single fibres was measured in order to calculate their cross-sectional area. The muscle fibres were stimulated by platinum plate electrodes placed parallel to the long axis of the fibre. For each fibre, a control force–frequency curve was obtained by giving 500-ms tetani between 1 Hz and 150 Hz at 1-min intervals and plotting the peak force against the frequency. After a 15-min rest period, the muscle was subjected to 50 tetani (300 ms, 70 Hz) applied at 2-s intervals. Thirty minutes afterwards, a second force–frequency curve was obtained. Fibres were left for a further 30 min and then fatigued by repeatedly stimulating them with 70-Hz, 300-ms tetani at 2-s intervals until force had declined to 40% of the initial value. A final force–frequency curve was obtained 30 min after the end of the fatiguing stimulation.

Measurement of myoplasmic $[Ca^{2+}]_i$ in single muscle fibres

Single muscle fibres were allowed to equilibrate for 30 min and then a reference 70-Hz, 300-ms tetanus was evoked. Next the fibre was pressure injected with the fluorescent indicator Indo-1 in order to measure myoplasmic free calcium, $[Ca^{2+}]_i$. The dye was excited with light at $360 \pm 5 \text{ nm}$ and the light emitted at $405 \pm 5 \text{ nm}$ and $495 \pm 5 \text{ nm}$ was measured with two photomultiplier tubes. The ratio (R) of the light emitted at 405 nm to that emitted at 495 nm was translated to $[Ca^{2+}]_i$ using the following equation:

$$[Ca^{2+}]_i = K_D \beta (R - R_{min})(R_{max} - R)^{-1} \quad (1)$$

where K_D is the apparent dissociation constant of the dye (283 nM, measured intracellularly), β is the ratio of the 495-nm signals at very low and saturating $[Ca^{2+}]_i$, and R_{min} and R_{max} are the ratios at very low and at saturating $[Ca^{2+}]_i$, respectively (for further details see [2, 12]). Following injection of Indo-1, fibres were left for a further 30 min before any measurements were made.

Basal $[Ca^{2+}]_i$ was defined as the mean $[Ca^{2+}]_i$ during the 100 ms preceding a tetanus. Tetanic $[Ca^{2+}]_i$ was defined as the mean $[Ca^{2+}]_i$ measured during the last 100 ms of stimulation in each tetanus. Changes in the removal of Ca^{2+} by the SR were monitored by measuring the mean $[Ca^{2+}]_i$ over a 100-ms period (50–150 ms)

after the end of stimulation during the decay phase of the tetanic Ca^{2+} transient. Force–calcium curves were plotted as the force measured during the last 100 ms of stimulation in tetani at each frequency against the $[Ca^{2+}]_i$ measured during the same time period. These data were then fitted with the following Hill equation:

$$P = (P_{max} [Ca^{2+}]_i^N) / (Ca_{50}^N + [Ca^{2+}]_i^N)^{-1} \quad (2)$$

where P is the relative tetanic force, P_{max} the calculated peak tetanic force, Ca_{50} is the $[Ca^{2+}]_i$ which gives 50% of P_{max} , and N a measure of the slope of the relationship.

Solutions

Muscle preparations were superfused with a solution containing (in mmol l^{-1}): NaCl 121, KCl 5, $MgCl_2$ 0.5, Na_2HPO_4 0.4, $CaCl_2$ 1.8, EDTA 0.1, $NaHCO_3$ 24, glucose 5.5 and foetal calf serum (0.2%, Gibco). This solution was bubbled with 95% O_2 /5% CO_2 (pH 7.4). All experiments were performed at room temperature (24–26°C).

Statistics

Values are expressed as mean \pm SEM. A Student's unpaired t -test and $P < 0.05$ was used to check for statistical significance.

Results

Whole muscle basic contractile properties

The optimal lengths at which muscles generated maximum tetanic force (P_0) were similar (WT: $11.5 \pm 0.3 \text{ mm}$ and *ob/ob*: $11.0 \pm 0.3 \text{ mm}$). Muscle weights were significantly less in *ob/ob* than WT EDL muscles, being $10.7 \pm 0.7 \text{ mg}$ and $16.8 \pm 0.4 \text{ mg}$, respectively ($P < 0.05$). This was reflected in the mean force at 150 Hz measured in *ob/ob* EDL muscles being $212.3 \pm 22.9 \text{ mN}$, which was significantly less than that in WT EDL muscles, $307.6 \pm 17.5 \text{ mN}$ ($P < 0.05$). However, when the force was normalised to cross-sectional area, the normalised maximum tetanic force evoked by 150 Hz was similar in *ob/ob* and WT muscles (Table 1). The half-relaxation time of tetanic contractions was significantly greater in rested *ob/ob* muscles compared to rested WT muscles (Table 1).

Whole muscle contractile changes during and after a bout of activity

During a series of 50 tetani, tetanic force decreased to the same extent in the two groups (Table 1). In both the *ob/ob*

Table 1 Tetanic contraction properties in the extensor digitorum longus (EDL) muscle in the first and last tetanus of a series of 50 tetani. Values are mean \pm SEM of six muscles

	Wildtype	<i>ob/ob</i>
Measured peak tetanic force (kPa)	199.4 \pm 14.6	211.7 \pm 10.1
Half-relaxation time first (ms)	28.8 \pm 2.6	39.2 \pm 3.8*
Half-relaxation time last (ms)	115.3 \pm 17.8	122.0 \pm 7.0
Force loss (%)	61.2 \pm 1.4	59.5 \pm 1.3

* $P < 0.05$

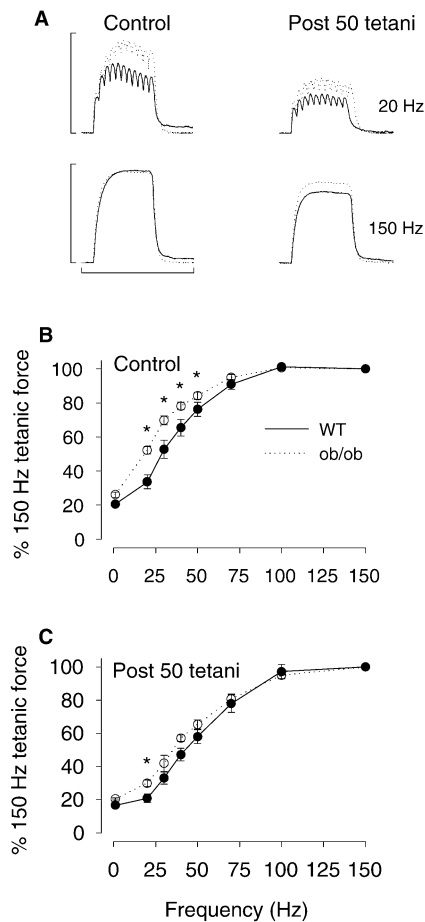


Fig. 1 **A** Typical force responses to a 500-ms tetanus at 20 Hz and 150 Hz in an extensor digitorum longus (EDL) muscle from an *ob/ob* (dotted line) muscle and wildtype (WT) (solid line) muscle under control conditions (Control) and 30 min after 50 tetani (Post 50 tetani). Horizontal calibration bar is 1 s and the vertical bar is 120 kPa at 20 Hz and 225 kPa at 150 Hz. **B** Force-frequency curves recorded from the EDL muscle of *ob/ob* mice or WT mice at rest. **C** Force-frequency curves recorded from the same muscles 30 min after the end of a series of 50 tetanic contractions (bottom). Values are mean \pm SEM of six muscles in each case. An asterisk indicates significant differences between *ob/ob* and WT; $P < 0.05$

and WT groups, contractions became progressively slower during the series of 50 tetani. Thus, the half-relaxation time of the last tetanus was three and four times longer than that of the first tetanus in the *ob/ob* and WT groups, respectively (Table 1).

Typical force records obtained at 20 Hz and 150 Hz before and 30 min after the series of 50 tetani are shown in Fig. 1A. In the rested muscles, force production was significantly greater at 20–50 Hz, ($P < 0.05$) in the *ob/ob* group than in the WT group (Fig. 1B). When the force-frequency curves were repeated 30 min after the end of 50 tetani, force production at low frequencies in both groups was considerably less than in the rested muscles, i.e. low-frequency fatigue was present. Force production was now significantly greater in the *ob/ob* group compared to the WT group only at 20 Hz (Fig. 1C).

Table 2 Tetanic contraction properties in single toe muscle fibres in the first and last tetanus of a series of 50 tetani. Values are mean \pm SEM of eight fibres (P_{\max} peak tetanic force)

	Wildtype	<i>ob/ob</i>
Measured peak tetanic force (kPa)	386.6 \pm 11.4	371.2 \pm 16.9
Half-relaxation time first tetanus (ms)	42.5 \pm 4.6	64.4 \pm 6.9*
Half-relaxation time last tetanus (ms)	57.4 \pm 6.3	99.0 \pm 13.4*
Force loss (%)	24.4 \pm 4.2	38.1 \pm 5.3
Calculated P_{\max} (kPa)	384 \pm 11	358 \pm 17
Ca_{50} (nM)	761 \pm 114	507 \pm 92
N (dimensionless)	2.93 \pm 0.28	4.25 \pm 1.02

* $P < 0.05$

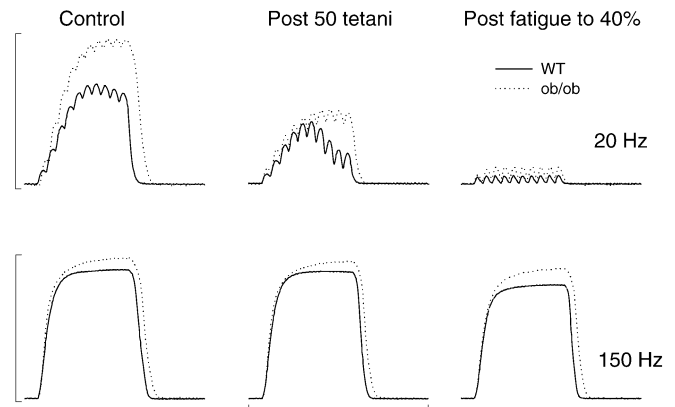


Fig. 2 Typical force responses to a 500-ms tetanus at 20 Hz and 150 Hz from an *ob/ob* muscle fibre and WT muscle fibre under control conditions (Control), 30 min after 50 tetani (Post 50 tetani) or 30 min post fatigue (Post fatigue to 40%). Dotted lines represent data from the *ob/ob* fibre and solid line data from the WT fibre. Horizontal calibration bar is 1 s and the vertical bar represents 320 kPa at 20 Hz and 450 kPa at 150 Hz

These results show that normalised force production was not less in *ob/ob* muscles than in WT muscles. In addition, *ob/ob* muscles did not fatigue more easily nor do they show greater low-frequency fatigue during recovery than their WT counterparts under the experimental conditions used here.

Single fibre basic contractile properties

Normalised force production was not significantly different between the two groups (Table 2). Typical force records obtained at 20 Hz and 150 Hz before, 30 min after a series of 50 tetani, and 30 min after fatigue to 40% of the initial force are shown in Fig. 2. It can be seen that 30 min after either 50 tetani or fatigue to 40%, force was markedly reduced at 20 Hz but was little affected at 150 Hz. Figure 3A shows the force-frequency response curve of *ob/ob* and WT single toe muscle fibres in the rested state. Force production in the *ob/ob* fibres was significantly greater than that in WT fibres at 30 Hz and 40 Hz. Force-calcium curves were calculated (see Materials and methods) for fibres in the two groups.

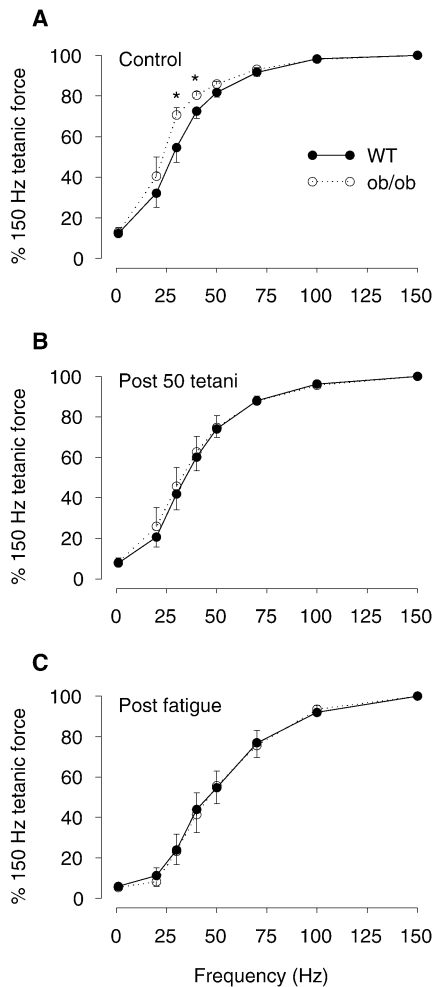


Fig. 3 Force-frequency curves recorded from single muscle fibres of *ob/ob* mice (dotted line) or WT mice (solid line) at rest (A), 30 min after the end of a series of 50 tetanic contractions (B) and 30 min after fibres had been fatigued (C). Values are mean \pm SEM of the same eight muscle fibres in each case. An asterisk indicates a value is significantly different from the WT value; $P < 0.05$

P_{max} , Ca_{50} and N were not significantly different between the two groups and were similar to values reported previously for toe muscle fibres [2, 12], indicating that the Ca^{2+} sensitivity of the myofilaments was similar (Table 2).

Single fibre $[Ca^{2+}]_i$ and force changes during and after 50 tetani

In the resting muscle fibres, the mean $[Ca^{2+}]_i$ was not significantly different in the two groups, being 73 ± 15 nM and 94 ± 15 nM in the *ob/ob* and WT single muscle fibres, respectively. Figure 4 shows the typical changes in $[Ca^{2+}]_i$ and force in an *ob/ob* fibre and a WT fibre during a series of 50 tetani. During the initial part of the series, the changes in $[Ca^{2+}]_i$ and force were essentially the same in the two fibres. However, over the last 10 tetani of the series they behaved very differently especially in terms of $[Ca^{2+}]_i$. Basal $[Ca^{2+}]_i$ increased sharply in the *ob/ob* fibre

but not in the WT fibre (see Fig. 4, inset). The abrupt rise in basal $[Ca^{2+}]_i$ towards the end of the series was observed in six of the eight *ob/ob* fibres but in none of the eight WT fibres or in any previous study of repetitive contraction in single fibres carried out in this laboratory (e.g. [11, 32]). The mean increase in basal $[Ca^{2+}]_i$ in the *ob/ob* group was 160 ± 30 nM which was significantly greater than that found in the WT group, 59 ± 10 nM ($P < 0.05$). The rise in basal $[Ca^{2+}]_i$ was largely reversed within 10 s after the end of tetanic stimulation in all fibres. In the last tetanus of the series of 50 tetani, tetanic $[Ca^{2+}]_i$ had decreased significantly by 35% from 1.72 ± 0.31 μ M to 1.13 ± 0.65 μ M ($P < 0.05$) in the *ob/ob* group but was unchanged in the WT fibres, being 1.83 ± 0.12 μ M and 1.76 ± 0.18 μ M in the first and the last tetanus, respectively. Tetanic force fell by from 338.8 ± 12.7 kPa to 210.3 ± 19.7 kPa ($P < 0.05$) in the *ob/ob* group and from 333.7 ± 10.9 kPa to 252.9 ± 15.9 kPa ($P < 0.05$) in the WT group in the last compared to the first tetanus. This decline in force over the series of 50 tetani was not significantly different between groups (Table 2).

The force-frequency curves were repeated 30 min after the end of 50 tetani (Fig. 3B). In both groups, force production at low frequencies was significantly less than in the rested muscle fibres, i.e. low-frequency fatigue was present. However, there were no significant differences in force production at any frequency between the *ob/ob* group and the WT group.

Single fibre $[Ca^{2+}]_i$ and force changes during and after fatigue to 40% of the initial force

Fibres were then subjected to a more severe fatiguing protocol by stimulating them repetitively until force fell to 40% of its initial value. The average number of tetani required to reduce force to 40% was significantly less ($P < 0.05$) in the *ob/ob* group compared to the WT group, being 100 ± 4 and 174 ± 19 , respectively. The typical changes observed in $[Ca^{2+}]_i$ and force in an *ob/ob* and a WT fibre are shown in Fig. 5. Three striking features are apparent. First, in contrast to the first series of 50 tetani, there was now an increase in tetanic $[Ca^{2+}]_i$ over the first 50 tetani in both groups of fibres. Second, especially in the case of the *ob/ob* fibres, the decrease in the peak tetanic force over the first 50 tetani was far less than that seen in the first series of 50 tetani. Third, the abrupt rise in basal $[Ca^{2+}]_i$ observed in the *ob/ob* fibre towards the end of the first series of 50 tetani was now postponed and occurred much later in the stimulation period. It is striking that the greatest rate of rise in basal $[Ca^{2+}]_i$ in *ob/ob* fibres occurred in the final 10 tetani of the period of fatiguing stimulation, while in WT fibres basal $[Ca^{2+}]_i$ rose steadily during the period of stimulation (Fig. 5, inset). This rapid increase in basal $[Ca^{2+}]_i$ was observed in seven of the eight *ob/ob* fibres examined but in none of the eight WT fibres. It is noteworthy that the single *ob/ob* fibre which did not show any abrupt rise in basal $[Ca^{2+}]_i$ also failed to show any abrupt rise in $[Ca^{2+}]_i$ during the first period of stimulation with 50 tetani. The abrupt rise in basal $[Ca^{2+}]_i$

Fig. 4 Typical example of the changes in $[Ca^{2+}]_i$ (**A, B, C**) and force (**D, E**) of a single muscle fibre from an *ob/ob* mouse (**B** and **E**) or WT (**A** and **D**) mouse during a series of 50 70-Hz, 300-ms tetani applied at 2-s intervals. **C** Comparison of the changes in basal $[Ca^{2+}]_i$ in the two muscle fibres over the period of the last 25 tetani on an expanded scale

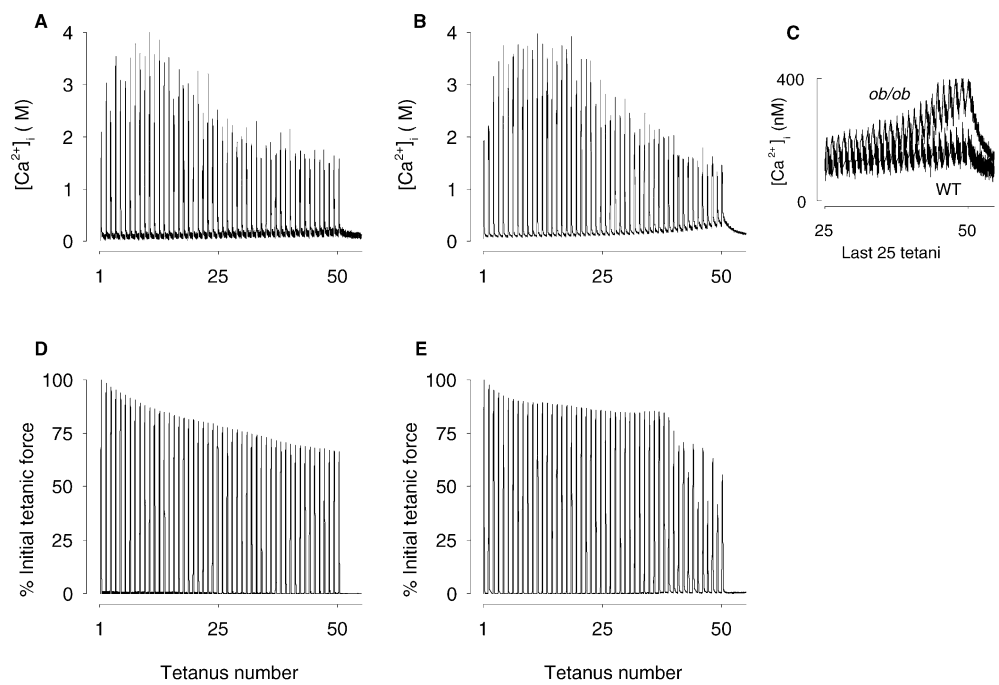
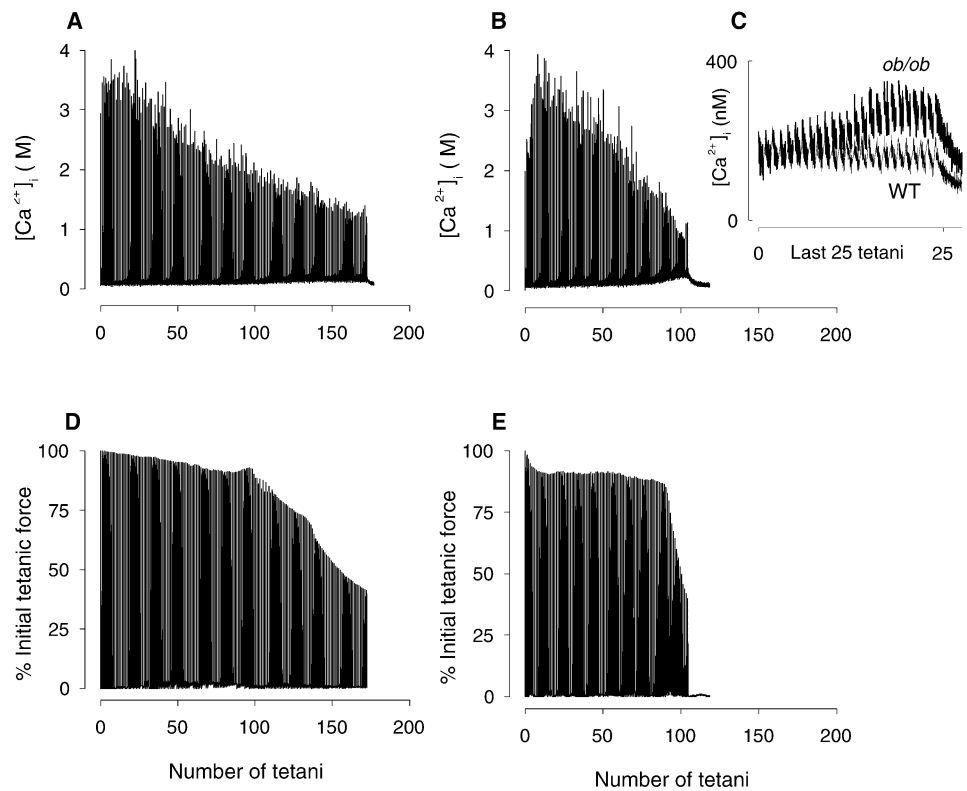


Fig. 5 Typical example of the changes in $[Ca^{2+}]_i$ (**A, B, C**) and force (**D, E**) of a single muscle fibre from an *ob/ob* mouse (**B** and **E**) or WT mouse (**A** and **D**) during a series of 70-Hz, 300-ms tetani applied at 2-s intervals until force had fallen to 40% of its initial value. **C** Comparison of the changes in basal $[Ca^{2+}]_i$ over the period of the last 25 tetani in the two muscle fibres on an expanded scale. The fibres shown here are the same as those shown in Fig. 4



also coincided with a rapid decline in both tetanic $[Ca^{2+}]_i$ and force in the *ob/ob* group (Fig. 6). The mean increase in basal $[Ca^{2+}]_i$ at the end of fatiguing stimulation was 166 ± 31 nM in the *ob/ob* group and 65 ± 21 nM in the WT group and these values were significantly different from each other ($P < 0.05$).

In previous studies of fatigue in single muscle fibres, it has been shown that basal $[Ca^{2+}]_i$ rises due to a slowing of calcium removal by the SR (e.g. [34]). A convenient method of estimating a decrease in Ca^{2+} removal by the SR is to measure $[Ca^{2+}]_i$ during the decay phase of the tetanic Ca^{2+} transient [33]. The decay $[Ca^{2+}]_i$ was

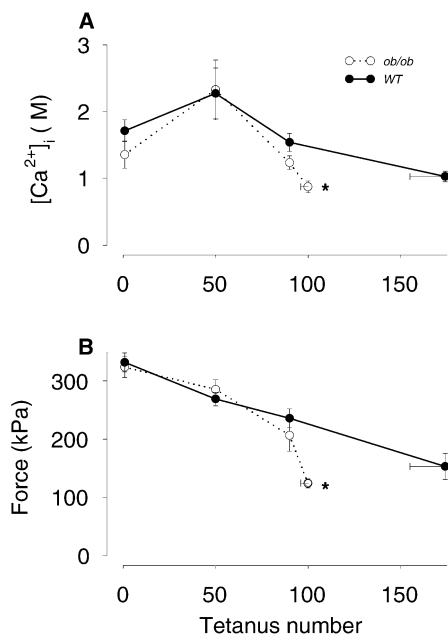


Fig. 6 Mean tetanic $[Ca^{2+}]_i$ (**A**) and force (**B**) of muscle fibres from *ob/ob* mice (dotted line and open symbol) or WT mouse (solid line and filled symbol) in the 1st, 50th, 90th and last tetanus of a series of 70-Hz, 300-ms tetani applied at 2-s intervals. All data points are mean \pm SEM of eight muscle fibres. Horizontal error bar indicates the SEM of the number of tetani required to reduce force to 40% of the initial value. An asterisk indicates value is significantly different from the WT value; $P < 0.05$

measured in the interval 50–150 ms after each tetanus. At the start of fatigue, decay $[Ca^{2+}]_i$ was 240 ± 30 nM and 244 ± 25 nM in the *ob/ob* and WT fibres, respectively. In the last tetanus when force had fallen to 40%, decay $[Ca^{2+}]_i$ was significantly increased to 395 ± 41 nM and 295 ± 24 nM in the *ob/ob* and WT fibres, respectively. The increase in decay $[Ca^{2+}]_i$ was significantly greater in the *ob/ob* than in the WT fibres. Thus, active uptake of Ca^{2+} into the SR was slowed to a greater extent in *ob/ob* fibres than in WT muscle fibres during the induction of fatigue.

Previously, it was shown that mitochondria in mouse toe muscle fibres from normal NMRI mice do not take up Ca^{2+} [18]. One possible mechanism underlying the sudden, sharp drop in tetanic $[Ca^{2+}]_i$ and force is that Ca^{2+} had accumulated in the mitochondria leading to impaired energy production and increased reactive oxygen species (ROS) production (see Discussion). We measured mitochondrial Ca^{2+} using laser confocal microscopy and the Ca^{2+} -sensitive dye Rhod-2 which preferentially loads into the mitochondria (see [18] for further details). However in all four *ob/ob* toe muscle fibres that were examined, mitochondrial Ca^{2+} was unchanged during the induction of fatigue (data not shown).

Finally, the force–frequency curves were repeated 30 min after the end of stimulation (Fig. 3C). In both groups, force production at low frequencies was considerably less than in the rested muscles (Fig. 3A) or 30 min after the series of 50 tetani (Fig. 3B), i.e. considerable

low-frequency fatigue was present. However, there were no significant differences in force production between the two groups, indicating that the same degree of low-frequency fatigue was present in *ob/ob* and WT muscle fibres.

Discussion

The major novel results of this study are as follows. First, single muscle fibres from *ob/ob* and WT mice generate similar tetanic forces when force is normalised to cross-sectional area but relaxation is slower in *ob/ob* than WT fibres. Second, in single muscle fibres subjected to repeated contractions, tetanic $[Ca^{2+}]_i$ and force decrease more rapidly and abruptly in fibres from *ob/ob* mice than WT mice. Third, following a bout of repeated activity, there was a similar rightward shift in the force–frequency curve of fibres from *ob/ob* and WT mice. Fourth, the maintenance of basal $[Ca^{2+}]_i$ during repeated tetanic stimulation appears to be less well regulated in muscle fibres from *ob/ob* mice than in WT fibres. Finally, a prior bout of activity improves both the maintenance of $[Ca^{2+}]_i$ and the endurance or fatigue resistance of *ob/ob* fibres in subsequent repeated contractions.

In the only previous report of force production in *ob/ob* muscle, it was found that peak tetanic force production of EDL muscles was not significantly different between *ob/ob* and WT groups [31]. The present study demonstrates that in the EDL muscle and also in single toe muscle fibres, normalised force production was similar in *ob/ob* and WT mice. It is notable that when force is normalised to take account of cross-sectional area, force generation in single fibres was greater (this study and [8, 12, 34]) than that measured in whole muscle preparations [31]. This may reflect the fact that single fibres consist solely of the contracting fibre and measurement of their cross-sectional area is not confounded by the presence of unseen connective tissue, capillaries or inter-fibre spaces such as occurs in whole muscle or even muscle strips.

Previously, it had been suggested that slower relaxation of contractions in muscle from *ob/ob* or STZ-treated mice might be due to impaired Ca^{2+} handling in diabetic compared to non-diabetic muscle [10, 31]. This hypothesis was never directly tested. In enzymatically isolated muscle fibres from agouti mice, which are both obese and insulin-resistant, resting $[Ca^{2+}]_i$ was found to be greater than in fibres isolated from non-agouti mice [35]. However these data should be treated with caution since their resting $[Ca^{2+}]_i$ in normal muscle fibres was markedly higher than that reported by other groups using a similar enzymatic procedure to isolate muscle fibres [1, 19]. Thus, the elevated $[Ca^{2+}]_i$ reported by Zemel et al. [35] could indicate either that the sarcolemma was more permeable to Ca^{2+} entry in the agouti mice or that it was more susceptible to damage during the enzymatic isolation of fibres. In the present study, basal $[Ca^{2+}]_i$ was not significantly different in *ob/ob* and WT fibres under control conditions and the values obtained are comparable

to those reported previously in mechanically isolated muscle fibres [2, 12]. Similarly, tetanic Ca^{2+} transients in non-fatigued single muscle fibres from *ob/ob* and WT mice were almost identical, with no significant difference in $[\text{Ca}^{2+}]_i$ during the decay phase of the Ca^{2+} transient. These findings suggest that Ca^{2+} handling mechanisms are similar in *ob/ob* and WT muscle under control conditions. Thus, there is little evidence to support the suggestion that the slower relaxation of force seen in this study and in previous studies is due to slower pumping of Ca^{2+} into the SR. Since Ca^{2+} handling is not the problem, it could be hypothesised that the slower relaxation of force in *ob/ob* fibres reflects an increased Ca^{2+} sensitivity of the myofilaments, i.e. the myofilaments can generate a given force at a lower $[\text{Ca}^{2+}]_i$. However, as Table 2 shows, while the Ca^{2+} sensitivity was higher in *ob/ob* fibres compared to WT fibres, the values were not significantly different. A similar lack of difference in Ca^{2+} sensitivity in muscle fibres from diabetic rats was seen in the only previous study which examined the problem [28]. Several alternative mechanisms including altered cytoskeletal proteins can be advanced but one that we favour is that the kinetics of cross-bridge detachment are slower in fibres from *ob/ob* muscle than those from normal muscle.

Muscle fibres from *ob/ob* mice were able to maintain basal $[\text{Ca}^{2+}]_i$ only for a limited period of repetitive stimulation. It was quite unexpected to see the sharp rise in basal $[\text{Ca}^{2+}]_i$ that occurred in the majority of *ob/ob* fibres towards the end of both series of repeated tetanic stimulation. Possible causes of the rise in basal $[\text{Ca}^{2+}]_i$ include a reduced re-uptake of Ca^{2+} by the SR, an increased leak of Ca^{2+} from the SR or an increased influx of Ca^{2+} across the sarcolemma. The timing of the sharp rise in basal Ca^{2+} coincided with a decline in the amplitude of the tetanic Ca^{2+} transient. Active re-uptake of Ca^{2+} into the SR is known to be slowed during fatigue and this contributes to a rise in basal $[\text{Ca}^{2+}]_i$ [34]. In the present study, this slowing was reflected in the increased $[\text{Ca}^{2+}]_i$ measured during the decay phase of the tetanic Ca^{2+} transient. It is important to note that the decay of the Ca^{2+} transient was considerably more slowed in seven of the eight *ob/ob* fibres when basal Ca^{2+} started to increase suddenly than in the WT fibres which never showed any abrupt rise in basal $[\text{Ca}^{2+}]_i$. The most parsimonious interpretation of these data is that a significantly greater inhibition of the SR Ca^{2+} pump during fatigue in *ob/ob* fibres compared to WT muscle fibres is a major contributor to the sudden rise in basal $[\text{Ca}^{2+}]_i$.

Towards the end of the induction of fatigue, both tetanic Ca^{2+} and tetanic force fell more rapidly in *ob/ob* fibres than in WT fibres. The decline in tetanic Ca^{2+} and force in skeletal muscle fibres is a characteristic feature of the latter stages of the development of fatigue [32, 34]. Repeated contractions result in an altered metabolite profile in the muscle fibre. Numerous recent studies have attempted to determine which metabolic changes in a working muscle are involved in the development of fatigue. It has long been known that intracellular pH is

lower in fatigued than rested muscle. Several groups have demonstrated that this fall in intracellular pH is not the cause of the decline of force that occurs during the development of fatigue [5, 17]. Another candidate resulting from the increased metabolic activity is the increased production of ROS. Both ROS and enzymes related to their elimination are elevated in resting diabetic muscle [13, 24]. It is known that ROS can exert powerful modulatory dose-dependent and time-dependent effects in skeletal muscle [2, 26, 29]. Further work is required to examine whether ROS are involved in the abrupt rise in basal $[\text{Ca}^{2+}]_i$ in *ob/ob* fibres during repeated tetanic contractions.

Recent data suggest that one or more of the following three factors play a major role in fatigue: decreased glycogen stores resulting in a failure of the energy supply [8], a decline in local [ATP] resulting in reduced release of Ca^{2+} from the SR [3] and a rise in inorganic phosphate which enters and precipitates with Ca^{2+} in the SR and thus reduces Ca^{2+} available for release [11, 25]. In the relatively few studies which have focused on the energetic changes in diabetic muscle, it has been reported that changes in glycogen, energy-rich phosphates and inorganic phosphate during repeated sub-maximal contractions are either similar [6] or else slightly greater in diabetic compared to normal muscle [7]. While no single study has investigated the changes in glycogen content in *ob/ob* muscle during repeated contractions, it is known that resting glycogen levels in *ob/ob* muscle are only half those in WT muscle [15]. It is possible that the lower glycogen content in *ob/ob* muscle contributes to the faster decline of tetanic Ca^{2+} and force in *ob/ob* fibres.

It is intriguing that the exercise-induced changes in basal and tetanic Ca^{2+} in *ob/ob* muscle fibres started after about 80 tetani in the second series of contractions compared to after only 40 tetani in the first series. It appears that the first bout of repetitive stimulation induced some degree of adaptation or training effect in the both groups but most obviously in the *ob/ob* muscle fibres. This adaptation endured much longer than the force potentiation resulting from light chain phosphorylation [30] or reduction of inorganic phosphate [4] reported after brief bouts of tetanic contraction. The mechanisms underlying this adaptation remain to be identified.

In summary, under resting conditions muscle fibres from *ob/ob* mice and normal mice show no major differences in basal $[\text{Ca}^{2+}]_i$ and tetanic Ca^{2+} transients. However, during a bout of repeated tetanic contractions, muscle fibres from *ob/ob* mice are less able to maintain their control of $[\text{Ca}^{2+}]_i$. This results in elevated basal $[\text{Ca}^{2+}]_i$, reduced tetanic $[\text{Ca}^{2+}]_i$ and premature fatigue. Interestingly, during a second series of contractions, muscle fibres from *ob/ob* mice showed a marked improvement in Ca^{2+} handling and maintenance of force.

Acknowledgements This work was supported by Novo Nordisk Fonden, The Swedish Research Council (project numbers 10842 and 14402), Swedish National Center for Sports Research and funds at the Karolinska Institute.

References

- Allard B, Bernengo JC, Rougier O, Jacquemond V (1996) Intracellular Ca^{2+} changes and Ca^{2+} -activated K^{+} channel activation induced by acetylcholine at the endplate of mouse skeletal muscle fibers. *J Physiol (Lond)* 494:337–349
- Andrade FH, Reid MB, Allen DG, Westerblad H (1998) Effect of hydrogen peroxide and dithiothreitol on contractile function of single skeletal muscle fibres from the mouse. *J Physiol (Lond)* 509:565–575
- Blazev R, Lamb GD (1999) Low [ATP] and elevated $[\text{Mg}^{2+}]$ reduce depolarization-induced Ca^{2+} release in rat skinned skeletal muscle fibres. *J Physiol (Lond)* 520:203–215
- Bruton JD, Wretman C, Katz A, Westerblad H (1997) Increased tetanic force and reduced myoplasmic $[\text{P}_i]$ following a brief series of tetani in mouse soleus muscle. *Am J Physiol* 272:C870–C874
- Bruton JD, Lännergren J, Westerblad H (1998) Effects of CO_2 -induced acidification on the fatigue resistance of single mouse muscle fibers at 28°C. *J Appl Physiol* 85:478–483
- Challiss RA, Vranic M, Radda GK (1989) Bioenergetic changes during contraction and recovery in diabetic rat skeletal muscle. *Am J Physiol* 256:E129–E137
- Challiss RA, Blackledge MJ, Radda GK (1990) Spatially resolved changes in diabetic rat skeletal muscle metabolism in vivo studied by 31P-nmr spectroscopy. *Biochem J* 268:111–115
- Chin ER, Allen DG (1997) Effects of reduced muscle glycogen concentration on force, Ca^{2+} release and contractile protein function in intact mouse skeletal muscle. *J Physiol (Lond)* 498:17–29
- Cotter M, Cameron NE, Lean DR, Robertson S (1989) Effects of long-term streptozotocin diabetes on the contractile and histochemical properties of rat muscles. *Q J Exp Physiol* 74:65–74
- Cotter MA, Cameron NE, Robertson S, Ewing I (1993) Polyol pathway-related skeletal muscle contractile and morphological abnormalities in diabetic rats. *Exp Physiol* 78:139–155
- Dahlstedt AJ, Katz A, Wieringa B, Westerblad H (2000) Is creatine kinase responsible for fatigue? Studies of isolated skeletal muscle deficient in creatine kinase. *FASEB J* 14:982–990
- Dahlstedt AJ, Katz A, Westerblad H (2001) Role of myoplasmic phosphate in contractile function of skeletal muscle: studies on creatine kinase-deficient mice. *J Physiol (Lond)* 533:379–388
- De Angelis KL, Cestari IA, Barp J, Dall'Ago P, Fernandes TG, Bittencourt PI de, Bello-Klein A, Bello AA, Llesuy S, Irigoyen MC (2000) Oxidative stress in the latissimus dorsi muscle of diabetic rats. *Braz J Med Biol Res* 33:1363–1368
- Eibschutz B, Lopaschuk GD, McNeill JH, Katz S (1984) Ca^{2+} -transport in skeletal muscle sarcoplasmic reticulum of the chronically diabetic rat. *Res. Commun Chem Pathol Pharmacol* 45:301–304
- Fosgerau K, Westergaard N, Quistorff B, Grønnet N, Kristiansen M, Lundgren K (2000) Kinetic and functional characterization of 1,4-dideoxy-1, 4-imino-*D*-arabinitol: a potent inhibitor of glycogen phosphorylase with anti-hyperglycaemic effect in *ob/ob* mice. *Arch Biochem Biophys* 380:274–284
- Ganguly PK, Mathur S, Gupta MP, Beamish RE, Dhalla NS (1986) Calcium pump activity of sarcoplasmic reticulum in diabetic rat skeletal muscle. *Am J Physiol* 251:E515–E523
- Lamb GD, Recupero E, Stephenson DG (1992) Effect of myoplasmic pH on excitation-contraction coupling in skeletal muscle fibres of the toad. *J Physiol (Lond)* 448:211–224
- Lännergren J, Westerblad H, Bruton JD (2001) Changes in mitochondrial Ca^{2+} detected with Rhod-2 in single frog and mouse skeletal muscle fibres during and after repeated tetanic contractions. *J Muscle Res Cell Motil* 22:265–275
- Leijendekker WJ, Passaquin AC, Metzinger L, Ruegg UT (1996) Regulation of cytosolic calcium in skeletal muscle cells of the *mdx* mouse under conditions of stress. *Br J Pharmacol* 118:611–616
- Le Marchand-Brustel Y, Jeanrenaud B, Freychet P (1978) Insulin binding and effects in isolated soleus muscle of lean and obese mice. *Am J Physiol* 234:E348–E358
- Levy J (1999) Abnormal cell calcium homeostasis in type 2 diabetes mellitus: a new look on old disease. *Endocrine* 10:1–6
- McGuire M, MacDermott M (1998) The influence of streptozotocin-induced diabetes and the antihyperglycaemic agent metformin on the contractile characteristics and the membrane potential of the rat diaphragm. *Exp Physiol* 83:481–487
- McGuire M, MacDermott M (1999) The influence of streptozotocin diabetes and metformin on erythrocyte volume and on the membrane potential and the contractile characteristics of the extensor digitorum longus and soleus muscles in rats. *Exp Physiol* 84:1051–1058
- Nakao C, Ookawara T, Sato Y, Kizaki T, Imazeki N, Matsubara O, Haga S, Suzuki K, Taniguchi N, Ohno H (2000) Extracellular superoxide dismutase in tissues from obese (*ob/ob*) mice. *Free Radic Res* 33:229–241
- Posterino GS, Fryer MW (1998) Mechanisms underlying phosphate-induced failure of Ca^{2+} release in single skinned skeletal muscle fibers of the rat. *J Physiol (Lond)* 512:97–108
- Reid MR (2001) Redox modulation of skeletal muscle contraction: what we know and what we don't. *J Appl Physiol* 90:724–731
- Shafir E (1992) Animal models of non-insulin-dependent diabetes. *Diabetes Metab Rev* 8:179–208
- Stephenson GM, O'Callaghan A, Stephenson DG (1994) Single-fiber study of contractile and biochemical properties of skeletal muscles in streptozotocin-induced diabetic rats. *Diabetes* 43:622–628
- Sun J, Xu L, Eu JP, Stamler JS, Meissner G (2001) Classes of thiols that influence the activity of the skeletal muscle calcium release channel. *J Biol Chem* 276:15625–15630
- Tubman LA, MacIntosh BR, Maki WA (1996) Myosin light chain phosphorylation and post-tetanic potentiation in fatigued skeletal muscle. *Pflugers Arch* 431:882–887
- Warmington SA, Tolan R, McBennett S (2000) Functional and histological characteristics of skeletal muscle and the effects of leptin in the genetically obese (*ob/ob*) mouse. *Int J Obes Relat Metab Disord* 24:1040–1050
- Westerblad H, Allen DG (1991) Changes of myoplasmic calcium concentration during fatigue in single mouse muscle fibers. *J Gen Physiol* 98:615–635
- Westerblad H, Allen DG (1994) The role of sarcoplasmic reticulum in relaxation of mouse muscle; effects of 2,5-di(tert-butyl)-1,4-benzohydroquinone. *J Physiol (Lond)* 474:291–301
- Westerblad H, Lännergren J, Allen DG (1997) Slowed relaxation in fatigued skeletal muscle fibers of *Xenopus* and mouse. Contribution of $[\text{Ca}^{2+}]_i$ and cross-bridges. *J Gen Physiol* 109:385–399
- Zemel MB, Kim JH, Woychik RP, Michaud EJ, Kadwell SH, Patel IR, Wilkison WO (1995) Agouti regulation of intracellular calcium: role in the insulin resistance of viable yellow mice. *Proc Natl Acad Sci USA* 92:4733–4737